Available online at www.sciencedirect.com
ScienceDirect
Clinical Biomechanics 23 (2008) 881–885
CLINICAL BIOMECHANICS
www.elsevier.com/locate/clinbiomech

Preliminary analysis of the forces on the thoracic cage of patients with pectus excavatum after the Nuss procedure

Pei Yeh Chang [a,*], Zhen-Yu Hsu [b], Da-Pan Chen [b], Jin-Yao Lai [a], Chao-Jan Wang [c]

[a] Department of Pediatric Surgery, Chang Gung Memorial Hospital, Chang Gung University, College of Medicine, Taoyuan, Taiwan
[b] Department of Mechanical Engineering, Chiao-Tung University, Hsinchu, Taiwan
[c] Department of Radiology, Chang Gung Memorial Hospital, Chang Gung University, College of Medicine, Taoyuan, Taiwan

Received 2 August 2007; accepted 19 February 2008

Abstract

Background. The Nuss procedure corrects pectus excavatum using a pre-bent bar that generates stress on the chest wall. To investigate the biomechanical effects after the Nuss procedure, we designed a three-dimensional finite element analysis model to analyze the distribution of stress and strain induced in the chest wall.

Methods. Three patients with pectus excavatum aged 8, 7, and 7 years, were enrolled in this study. The greatest upward displacements of their sternums after the operation were measured from computed tomography images and chest X-ray films. Based on these displacements, we constructed three finite element analysis models for analyzing biomechanical changes in the thoracic cage after the Nuss procedure.

Findings. The simulation results indicated that greatest strain occurred at the third through seventh cartilages, especially where they join the sternum and ribs. A high bilateral stress distribution was also found over the backs of the third to the seventh ribs near the vertebral column.

Interpretation. The stress and strain induced by the Nuss procedure can be analyzed using our finite element analysis model. Although the stress and strain may have some influence on chest and spine development, a more detailed finite element analysis model is recommended for future study to improve the accuracy of our simulation results.

Keywords: Finite element analysis; Pectus excavatum; Nuss procedure; Biomechanical simulation; Stress and strain

1. Introduction

Pectus excavatum (PE) is a common chest wall malformation (Fonkalsrud, 2003) thought to be caused by the excessive growth of the costal cartilage, which produces a concave anterior chest wall (Länsman et al., 2002). In 1998, Nuss introduced a minimally invasive technique for repairing PE (Nuss et al., 1998). In this procedure, the depression of the sternum is corrected by inserting a metal bar (a Nuss bar) under the sternum without removing the costal cartilage. Until recently, most research efforts have focused on improving the Nuss procedure (Nuss et al., 1998; Croitoru et al., 2002; Park et al., 2004b) and preventing complications (Hebra et al., 2000; Park et al., 2004a; Croitoru et al., 2005). However, little mention has been made about analyzing the biomechanical effects on the chest wall of patients with PE who have undergone the Nuss procedure. Because investigating the influence of the stress generated on the chest wall of these patients is extremely difficult, if not impossible, under clinical conditions, we developed a finite element analysis (FEA) model specifically to analyze the stress and the strain distributions induced in the chest wall by a Nuss procedure.

* Corresponding author.
E-mail address: pyjchang@cgmh.org.tw (P.Y. Chang).

0268-0033/$ - see front matter © 2008 Elsevier Ltd. All rights reserved.
doi:10.1016/j.clinbiomech.2008.02.010

2. Methods

2.1. Patient-specific finite element models

The Nuss procedure is an evident biomechanical manipulation of the chest wall caused by the insertion of a metal bar. From our clinical observations, the deformation after the Nuss procedure is different for each patient with PE. FEA models must be generated individually to ensure the possible application of simulated results. It was not our intention to construct a general model of the biomechanical effects for application to all patients.

We carefully chose three symmetric types of patients with PE (Park et al., 2004b) for our study to eliminate the factors due to asymmetric configuration of the chest wall. The patients were 8, 7, and 7 years old, and their pectus indexes were 5.3, 4.7, and 5.2, respectively (Table 1). The first and the third patients were boys and the second was a girl. All of these patients had a preoperative computed tomography (CT) scan, and a chest X-ray taken immediately after the operation. The CT studies were performed with a 16-slice scanner (Siemens SOMATOM Sensation 16) using the protocol described in our previous study (Chang et al., 2006, 2007). Informed consent was obtained from the guardian of each patient, and this study was approved by our hospital's ethics committee (CGMH: IRB 94-934B).

An appropriately simplified FEA model is necessary for a complicated analysis such as this to ensure that the model is easily reproducible while still generating useful ideas to check the possible implications and complications of the operation. Our FEA models consisted of the ribs, sternum, and costal cartilage, which provide the major contributions to rib cage integrity. Since the contributions to the chest wall integrity of the muscles and skin were much less than those of the bone and cartilage, we ignored those components in our study (Yang and Wang, 1998; Gignac et al., 2000; Feng et al., 2001). Moreover, based on our clinical observations, the shape of the vertebral column of each of the three patients did not significantly change after the Nuss procedure. Therefore, the displacement of the joints between the rib and spine was assumed to be constant, and the vertebral columns were not included in our rib cage models.

Since the grayscale value of costal cartilage was indistinct from other tissues on the CT slices, the automatic segmentation of cartilage by the AMIRA visualization software was incomplete. To overcome this problem, we developed a semiautomatic procedure for reconstructing the rib cage model. First, the CT slices were imported into AMIRA, and the segments of the rib, sternum, and costal cartilage were labeled automatically by assigning respective grayscale values to them. Then, the segments of costal cartilage were modified manually. These segment modifications relied on our professional experience.

After the geometric models were created, the FEA models were generated with tetrahedral elements using AMIRA. A convergence test was performed to confirm the simulated accuracy of the mesh by comparing the simulated results of six rib cage meshes (Table 2). The convergence criterion was that the difference in the corrected displacement at the end of the sternum was less than 1%, and the final choice was a FEA model that consisted of approximately 320,000 tetrahedral elements.

Table 1
Biomechanical data from the three simulations of the Nuss procedure

	Case 1	Case 2	Case 3
Sex/age	M[b]/8	F[b]/7	M[b]/7
Pectus index	5.3	4.7	5.2
Elevation of the end of sternum (cm)[a]	4.47	3.40	3.90
Simulation results:			
1. Simulation displacement at the end of the sternum (cm)	4.49	3.43	3.90
2. Loading force at the end of the sternum (N)	140	120	190
3. Maximal stress at the end of the third rib near the spine (MPa)	24.89	48.50	33.25
4. Elongation of the right fourth cartilage (%)	4.30	5.74	5.26

[a] The elevation at the end of the sternum was measured as the difference in distance from the inner margin of the sternal end to the anterior surface of the vertebral body based on the preoperative CT scan and postoperative X-ray film.
[b] M, male; F, female.

2.2. Finite element analysis

The material properties of bone and cartilage were based on previous articles (Granik and Stein, 1973; Yang and Wang, 1998), and an elastic modulus of 11.5×10^9 Pa was chosen for the ribs and sternum. We assumed a value of 12.25×10^6 Pa for the pectus costal cartilages, which was about half the value of normal cartilage, as suggested by Feng et al. (2001). The material properties of the ribs, sternum, and costal cartilage were modeled as linear, as described by Murakami et al. (2006) and Roberts et al. (2005). During the Nuss procedure, the concave side of the Nuss bar was placed under the sternum and then forcibly turned and rotated to raise the depression of the sternum. Although this turning process may cause some damage to the chest wall, we ignored it in our analysis.

Table 2
Convergence test of six rib cage meshes

Number of elements	97,939	170,660	223,522	269,163	320,519	443,470
Corrected displacement at the end of the sternum	4.304	4.370	4.417	4.462	4.490	4.519
Mean difference (%)		1.5381	1.064	1.035	0.619	0.649

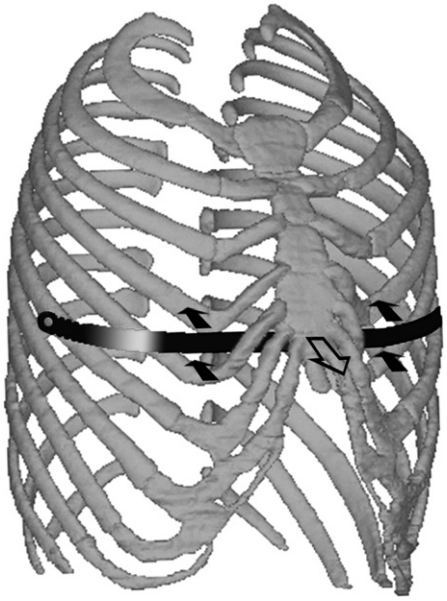

Fig. 1. Finite element pectus excavatum model corrected using a Nuss bar. The hollow arrow indicates F_e and the solid arrows denote F_{sr}.

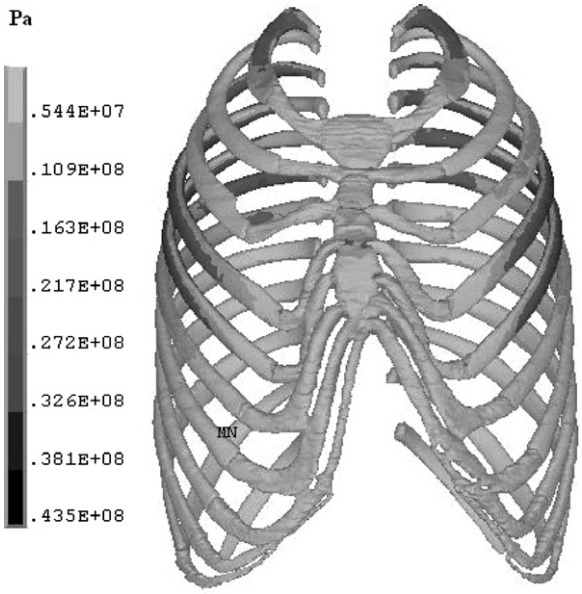

Fig. 2. Stress distribution with a 140-N elevating force for the model of patient 1.

After the depression of the sternum was completely raised by the Nuss bar, several reaction forces were generated on the chest wall. The Nuss bar provided an elevating force (F_e) to raise the depressed sternum. To preserve the equilibrium of the Nuss bar, two supporting forces (F_s) were generated simultaneously on each exit of the intercostal muscle, and the forces were transmitted to the ribs immediately above and below the exits as shown in Fig. 1. The forces applied to the ribs are called rib support forces (F_{sr}). Although these forces cannot be measured directly on the patients, it is reasonable to assume that they are equally distributed and the total of the rib supporting forces should be equivalent to the elevating force, i.e., $F_e = 2\ F_s = 4\ F_{sr}$. The locations of F_e and F_s were obtained from the chest X-rays taken after the operation. We developed our FEA models based on these assumptions. Moreover, since the corrected displacements at the end of the sternum in our patients were greater than 3.4 cm, we used the large displacement nonlinear solution in the ANSYS FEA software to ensure the accuracy of our simulation results.

3. Results

Table 1 shows the results of the FEA for our three patients. The actual upward displacements of the lowest points of sternum were measured from the CT scans taken before the Nuss procedure and from the chest X-rays taken after the procedure. These displacements were 4.47, 3.40, and 3.90 cm for the 8-, 7-, and 7-year-old patients, respectively. Fig. 2 shows the stress distribution of the first model under the loading of a 140-N elevating force. The stress is concentrated on the third through the seventh ribs and apparently higher on the back than on the front. Fig. 3 shows the strain distribution of the first model. The deformation of the costal cartilage is larger than the deformation of the ribs and the sternum, while the maximum strain is focused on the bilateral third to seventh cartilage junctions with the sternum and the ribs. Similar results were found in patients 2 and 3 as shown in Table 1. The elongation of the right fourth cartilage, which represented a larger strain area after the procedure, is also shown in Table 1.

4. Discussion

We analyzed three FEA models of the thoracic cage of PE patients. These models were a simplified representation of the human body to investigate biomechanical effects that cannot be studied clinically in a patient with PE after a Nuss procedure. Fonkalsrud and Reemtsen (2002) studied four children with PE younger than 11 years old, and found that the average force required to raise their sternums to the normal position was 68.1 N. Weber et al. (2006) determined that the force required to correct PE for male patients aged 5–17 years was 181 ± 48.3 N. The amount of force in our simulation was quite similar to those two studies. The similarity between the postoperative chest images and our simulation also confirms the validity of our study.

Since no removal of costal cartilage occurs during a Nuss procedure, the elevating force applied to the sternum will generate a corresponding stress that is transmitted to the entire chest wall through the sternum, the cartilage, and the ribs. According to our simulation results, the strain on the costal cartilages was greater than on the bony ribs after the sunken sternum was raised completely. Higher strains were focused on the joints of the cartilage with its corresponding bony rib and the sternum. However, the

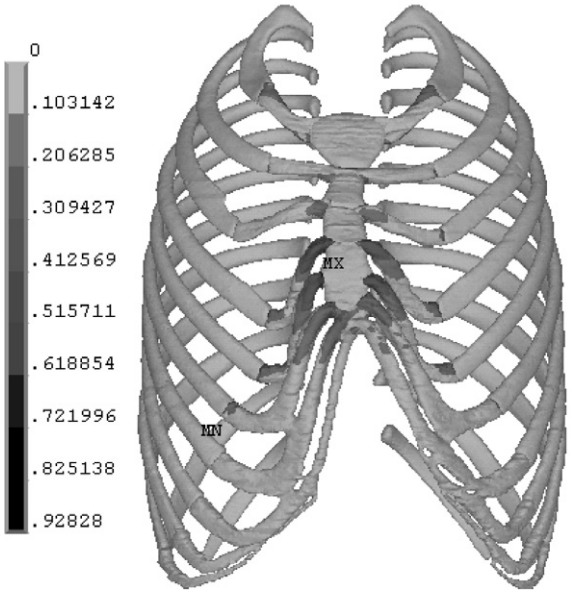

Fig. 3. Strain distribution with the same force for the model of patient 1.

stress distribution in Fig. 1 indicates that a greater stress level was generated on the backs of the patients, and concentrated bilaterally on the third through seventh ribs. The back-end strain values on the ribs were smaller than the strain values on the cartilage. In Fig. 2, the largest strain on the costal cartilage was 93 times the strain on the bony rib (0.928 versus 0.01). The elasticity modulus of the rib and costal cartilage were 11.5 GPa and 12.25 MPa, respectively; i.e., the elasticity modulus of the rib was 938 times that of the costal cartilages. Based on the fundamental elasticity equation $\sigma = E\varepsilon$, where σ is the stress, E is the modulus of elasticity, and ε is the strain of a mechanical system (Shigley and Mischke, 2001), the stress applied on the rib would be about 10.12 times that on the costal cartilage. Therefore, a greater level of stress was generated on the backs of the patients than on the cartilage.

We carefully studied human cartilage specimens from patients with PE. The fracture load in the pectus cartilage was less than the fracture load in the control group both in tension and in compression (Feng et al., 2001). The magnitude of the strain could break the costocartilage joints instead of fracturing the cartilage. After elevating the end of the sternum, micro-damage of the ribs in contact with the bar and at the costochondral junctions was reported recently by Ohno et al. (2006). This finding was for patients generally older than the age of 9 years. Waters et al. (1989) stated that asymmetric pneumatic thoracic pressures and paraspinal muscle imbalance might be the cause of scoliosis associated with PE. With some asymmetric deformity in the thoracic cage of patients with PE, thoracic scoliosis might be induced by the stress on the back of the ribs after a Nuss procedure, as observed by Niedbala et al. (2003). In his report, two patients were found to have developed thoracic scoliosis after the Nuss procedure. Importantly, the second patient developed temporary thoracic scoliosis at the third through the seventh thoracic spines, which are precisely the areas our simulated results identified as having the highest stress.

With an improved FEA model, we expect our simulation to provide valuable information on the specific design details of a Nuss procedure before the actual operation. This could include an optimal Nuss bar shape to produce minimal stress and strain, the location of the best elevation for the Nuss bar, and whether one or two bars should be used. Since the geometric models were based on the CT scan data, they are limited by the amount of detail that the CT images provide. If we neglect the minimal error from the CT scan system, the accuracy of the model is decided by the pixel space and the interval between each slice. A smaller space and interval will enhance the accuracy of model. In this study, the pixel space and interval were 0.40625 mm and 0.7 mm, respectively. We believe that less manipulation by modelers will be required as CT technology advances.

5. Conclusions

The stress and strain induced by the Nuss procedure can be analyzed with our biomechanical model. Although the procedure has some influence on the development of the chest and spine, the accuracy of the reconstructed geometric model and the underlying assumptions of our simplified FEA model may affect the accuracy of the simulation results. Moreover, the complexity of the interactions among the spine, the muscles, and the skin should be considered to improve the accuracy and utility of this analysis.

Conflict of interest

None of us has financial or personal relationships with people or organizations that could inappropriately influence our work.

Acknowledgements

This study was supported by the National Center for High-Performance Computing (NCHC), Hsinchu, Taiwan. We thank Dr. Lun-Jou Lo at Chang Gung Memorial Hospital (Taoyuan, Taiwan, ROC) for his assistance in creating the FEA models reported in this paper.

References

Chang, P.Y., Lai, J.Y., Chen, J.C., Wang, C.J., 2006. The long-term changes of the bone and cartilage after Ravitch's thoracoplasty: identification with multislice CT with 3D reconstruction. J. Pediatr. Surg. 41, 1947–1950.

Chang, P.Y., Lai, J.Y., Chen, J.C., Wang, C.J., 2007. Quantitative evaluation of bone and cartilage changes after the Ravitch thoracoplasty by multislice computed tomography with 3-dimensional reconstruction. J. Thorac. Cardiovasc. Surg. 134, 1279–1283.

Croitoru, D.P., Kelly Jr., R.E., Goretsky, M.J., Lawson, M.L., Swoveland, B., Nuss, D., 2002. Experience and modification update for the

minimally invasive Nuss technique for pectus excavatum repair in 303 patients. J. Pediatr. Surg. 37, 437–445.

Croitoru, D.P., Kelly Jr., R.E., Goretsky, M.J., Gustin, T., Keever, R., Nuss, D., 2005. The minimally invasive Nuss technique for recurrent or failed pectus excavatum repair in 50 patients. J. Pediatr. Surg. 40, 181–187.

Feng, J., Hu, T., Liu, W., Zhang, S., Tang, Y., Chen, R., Jiang, X., Wei, F., 2001. The biomechanical, morphologic, and histochemical properties of the costal cartilages in children with pectus excavatum. J. Pediatr. Surg. 36, 1770–1776.

Fonkalsrud, E.W., 2003. Current management of pectus excavatum. World J. Surg. 27, 502–508.

Fonkalsrud, E.W., Reemtsen, B., 2002. Force required to elevate the sternum of pectus excavatum patients. J. Am. Coll. Surg. 195, 575–577.

Gignac, D., Aubin, C.-É., Dansereau, J., Labelle, H., 2000. Optimization method for 3D bracing correction of scoliosis using a finite element model. Eur. Spine J. 9, 185–190.

Granik, G., Stein, I., 1973. Human ribs: static testing as a promising medical application. J. Biomech. 6, 237–240.

Hebra, A., Swoveland, B., Egbert, M., Tagge, E.P., Georgeson, K., Othersen Jr., H.B., Nuss, D., 2000. Outcome analysis of minimally invasive repair of pectus excavatum: review of 251 cases. J. Pediatr. Surg. 35, 252–258.

Länsman, S., Serlo, W., Linna, O., Pohjonen, T., Törmälä, P., Waris, T., Ashammakhi, N., 2002. Treatment of pectus excavatum with bioabsorbable polylactide plates: preliminary results. J. Pediatr. Surg. 37, 1281–1286.

Murakami, D., Kobayashi, S., Torigaki, T., 2006. Finite element analysis of hard and soft tissue contributions to thoracic response: sensitivity analysis of fluctuations in boundary conditions. Stapp Car Crash J. 50, 169–189.

Niedbala, A., Adams, M., Boswell, W.C., Considine, J.M., 2003. Acquired thoracic scoliosis following minimally invasive repair of pectus excavatum. Am. Surg. 69, 530–533.

Nuss, D., Kelly Jr., R.E., Croitoru, D.P., Katz, M.E., 1998. A 10-year review of a minimally invasive technique for the correction of pectus excavatum. J. Pediatr. Surg. 33, 545–552.

Ohno, K., Morotomi, Y., Harumoto, M., Ueda, M., Nakahira, M., Nakamura, T., Azuma, T., Moriuchi, T., Yoshida, T., Shiokawa, C., Nakaoka, T., 2006. Preliminary study on the effects of bar placement on the thorax after the Nuss procedure for pectus excavatum using bone scintigraphy. Eur. J. Pediatr. Surg. 16, 155–159.

Park, H.J., Lee, S.Y., Lee, C.S., 2004a. Complications associated with the Nuss procedure: analysis of risk factors and suggested measures for prevention of complications. J. Pediatr. Surg. 39, 391–395.

Park, H.J., Lee, S.Y., Lee, C.S., Youm, W., Lee, K.R., 2004b. The Nuss procedure for pectus excavatum: evolution of techniques and early results on 322 patients. Ann. Thorac. Surg. 77, 289–295.

Roberts, J.C., Biermann, P.J., O'Connor, J.V., Ward, E.E., Cain, R.P., Carkhuff, B.G., Merkle, A.C., 2005. Modeling nonpenetrating ballistic impact on a human torso. Johns Hopkins APL Tech. Dig. 26, 84–92.

Shigley, J.E., Mischke, C.R., 2001. Mechanical Engineering Design, sixth ed. McGraw-Hill, New York, NY, 103 pp.

Waters, P., Welch, K., Micheli, L.J., Shamberger, R., Hall, J.E., 1989. Scoliosis in children with pectus excavatum and pectus carinatum. J. Pediatr. Orthop. 9, 551–556.

Weber, P.G., Huemmer, H.P., Reingruber, B., 2006. Forces to be overcome in correction of pectus excavatum. J. Thoracic Cardiovasc. Surg. 132, 1369–1373.

Yang, K.H., Wang, K.H., 1998. Finite element modeling of the human thorax. In: Presented at the Second Visible Human Project Conference, Bethesda, MD, October 1–2.